Equivalent Circuit Simulation of Transverse Nonlinear Vibration of a Single-Axis Bogie

Feng HAO, Zheng WANG[1], Zhen BAO, Ping XU, Yuanpeng LEI and Sheng WANG
School of Mechatronic Engineering, Lanzhou Jiaotong University,
Lanzhou 730070, China

Abstract. Numerical simulation of non-linear vibration systems requires efficient programs and high performance computers as a means to improve computational efficiency. Based on the similarity between the mechanical system dynamics model and the simulated integral circuit, an equivalent circuit model of a 2-degree-of-freedom elastic single wheel pair with transverse non-linear vibration considering the wheel-rail gap is established, and the circuit model is simulated and analysed using Multisim. The results of the study show that the equivalent circuit simulation is consistent with the numerical simulation analysis results, except that the equivalent circuit simulation is fast and efficient overall, and the parameters can be modified in real time during the simulation run to dynamically observe the simulation analysis process. Equivalent circuit simulation provides a viable and efficient reference method for the study of non-linear system dynamics.

Keywords. nonlinear vibration, mechanical systems, equivalent circuit simulation, numerical simulation, dynamics

1. Introduction

With Lorenz's discovery of chaos in a simple three-dimensional space, many scholars have also discovered chaos in autonomous ordinary differential equations with quadratic nonlinearities, chaos is an inherent characteristic of nonlinear dynamic systems and a common phenomenon in nonlinear systems.[1,2]. As the research on nonlinearity deepened, there were more and more applications of circuits to implement nonlinear systems of equations, the most representative of which is the Chua's circuit, it can exhibit standard chaotic theoretical behavior[3,4,5]. The applied circuit model is similar to the dynamical model and has good similar properties for analysing phenomena caused by non-linear factors in dynamics.

The stability of a linear system depends only on its own properties, i.e. mass, damping and stiffness, and is independent of the external input signal, so it can be judged by determining whether the real part of the eigenvalues of its equation of state is less than zero. Especially in the case of computer numerical calculation of eigenvalues, the calculation is fast and the judgement is relatively simple. In contrast, the stability of a non-linear system depends not only on its own characteristics, but also on the input. At present, stability judgements are usually made using Lyapunov theory, by using this

---

[1] Corresponding Author, Zheng Wang; E-mail: wangz@stu.lzjtu.edu.cn.

method, stability can be directly determined without solving the system state equation. For nonlinear and time-varying systems, solving the state equation is often difficult, so the Lyapunov second method shows great superiority.[6,7,8] And the analysis of non-linear system vibrations is generally based on theoretical studies and numerical simulations, with numerical simulations being the most direct class of methods for vibration analysis, and calculations are usually realised using software such as MATLAB and C language [9,10,11]. However, when the system has large degrees of freedom, the numerical simulation requires the gradual integration of the differential equations of motion of the system, so it generates a huge amount of computation, which is accompanied by a large amount of time. In order to improve the efficiency of numerical simulation, the algorithm of the program is usually optimised or a high performance computer is used as a way to increase the speed of the computation [12,13,14].

To address this situation, numerical computational methods are applied to determine the eigenvalues of a multi-degree-of-freedom linear dynamics model so that the linear critical velocity in the dynamics of a vehicle system can be determined [15,16]. On this basis, the application software calculates the required resistance values in the equivalent circuit, given the equivalent circuit capacitance matrix, and designs a simulated integral equivalent circuit model exactly similar to the vehicle system dynamics. Since the difference between a non-linear system and a linear system in the actual model is only the non-linearisation of some of the parameters, a similar non-linear dynamics model is achieved by replacing some of the original linear parameters in the equivalent circuit with non-linear parameters, such as segmented linearity. On this basis, the excitation and response analysis of the model is used to achieve a non-linear analysis of the vehicle system dynamics model.

A gap of around 9 mm exists between the wheel rim of the rolling stock and the track, providing room for the automatic alignment of the wheel pair. When the vehicle runs at a high speed or travels on a curved line, the wheel pair will undergo a serpentine motion or deviate from the track centre line to one side, causing the track sides to come into contact with the wheel edge or even collide, forming a potential safety threat to the operation of the rolling stock [17,18,19,20]. Considering the characteristics of wheel-rail clearance and track elasticity as segmental linearity, a non-linear lateral dynamics model of an elastic single wheel pair containing wheel-rail clearance is established, based on the linear counterpart of the equivalent circuit with the addition of non-linear factors, and simulated in Multisim, the simulation results are compared with the numerical simulation, and the results are in good agreement, proving that the non-linear factors are added to the linear circuit to form a non-linear equivalent circuit. The method of realising the equivalence of a non-linear dynamical system is reasonable and feasible, and the equivalent circuit simulation has the advantages of real-time parameter adjustment by changing the resistance value and a relatively fast overall running time [21,22].

2. Dynamical Model of an Elastic Uniaxial Wheel Pair

Figure 1 shows a single axle wheel pair subjected to lateral and longitudinal elastic constraints. The spatial coordinate system XYZ is established with the origin O at the centre of a flat track, the X-axis is the direction of advancement of the wheel pair along the centre of the track, the Y-axis is the horizontal direction along the wheel axis and

the Z-axis is the direction perpendicular to the plane of the track. The track is fixed to the frame and the wheel pair is connected to the frame laterally by a linear spring Ky and a linear damping Cy, and longitudinally by a linear spring Kx and a linear damping Cx.
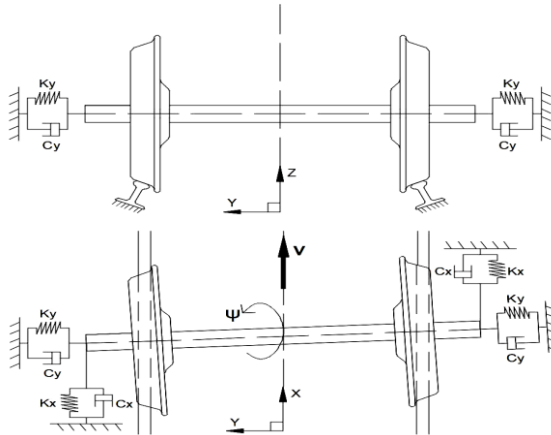

Figure 1. Diagram of flexible single wheel pair

When the rolling stock is in operation, the action between the wheels and rails is more complex, so Kalker's linear theory is chosen to facilitate the analytical calculation of the creep rate/force on the wheels and rails [2324,25], and the creep force on the wheel pair is:

$$
\begin{cases}
T_y = -f_{22}\zeta_1 = -f_{22}(\dfrac{\dot{y}_w}{V} - \psi_w) \\
T_x = -f_{11}\zeta_2 = -f_{11}(\dfrac{b\dot{\psi}_w}{V} - \dfrac{\lambda y_w}{r_0})
\end{cases}
\tag{1}
$$

In equation (1): T_y is the longitudinal creep slip force and T_x is the transverse creep slip force. Let y_w be the transverse displacement of the wheel pair, ψ_w be the angular displacement of the rocker of the wheel pair, V be the velocity of the wheel pair relative to the track, and f_{11} and f_{22} be the longitudinal and transverse creep slip coefficients respectively.

Neglecting the spin creep slip force and the higher order terms, and considering the gravitational stiffness, the elastic wheel pair dynamics equations are established based on the model in Figure 1 as follows:

$$
\begin{cases}
M\ddot{y}_w + (2C_y + \dfrac{2f_{22}}{V})\ \dot{y}_w + (2K_y + \dfrac{W\lambda}{b})\ y_w - 2f_{22}\psi_w = 0 \\
I\ddot{\psi}_w + (2C_x b_1^2 + \dfrac{2b^2 f_{11}}{V})\ \dot{\psi}_w + 2K_x b_1^2 \psi_w + \dfrac{2f_{11}b\lambda}{r_0} y_w = 0
\end{cases}
\tag{2}
$$

When the wheel pair is in the central position, the wheel edge is 9 mm away from the rail side, and when the lateral displacement of the vehicle is too large, this can lead to contact or even collision between the rail and the wheel edge, resulting in a large

wheel edge force between the wheels and rails. Due to the elasticity of the rail, this rim force is non-linear and the force is expressed as a segmented linear function as shown in Figure 2.
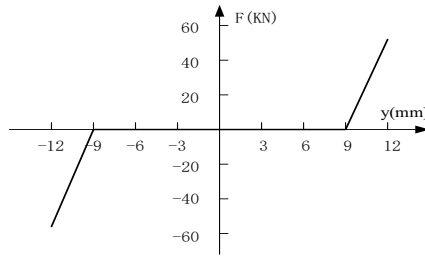

Figure 2. Segmented linear function of wheel edge forces

With the rail elasticity coefficient represented by k, the segmental linear descriptive equation is:

$$F_t(y) = \begin{cases} k(y-\eta) & y > \eta \\ 0 & |y| \le \eta \\ k(y+\eta) & y < -\eta \end{cases} \tag{3}$$

In formula (3), the wheel rim elasticity coefficient $k = 1.7 \times 10^7$ N/m; η is the wheel-rail clearance and is taken as $\eta = 0.009$ m.

3. Numerical Simulation

The elastic single wheelset of railway freight cars was selected for research, and its dynamic parameters are shown in Table 1:

Table 1. Kinetic parameters of the elastic single wheel pair

Wheel pair parameters	Numerical values
Mass M/kg	1500
Rotational inertia I/(kg·m^2)	1200
Equivalent taper λ	0.3
Axle half-length b/m	0.74
Half of left and right suspension distance b_1/m	1.05
Wheel radius r_0/m	0.44
Gravitational force W/kg	21600
Transverse stiffness K_y/(N·m^{-1})	2.4×10^6
Transverse damping C_y/(Ns·m^{-1})	2.2×10^4
Longitudinal stiffness K_x/(N·m^{-1})	2.8×10^6
Longitudinal damping C_x/(Ns·m^{-1})	2.2×10^4
Longitudinal creep-slip coefficient f_{11}/(N·m^{-1})	3.98×10^6
Transverse creep-slip coefficient f_{22}/(N·m^{-1})	3.62×10^6

Taking into account the case of non-linear rim forces generated when the rim is in contact with the rail, adding $F_t(y)$ to equation (1), it can be written as:

$$\begin{cases} m\ddot{y} + \dfrac{2f_{22}}{V}\dot{y} + (2K_y + \dfrac{W\lambda}{b})y - 2f_{22}\psi + F_t(y) = 0 \\ I\ddot{\psi} + \dfrac{2f_{11}b^2}{V}\dot{\psi} + 2K_x b^2 \psi + \dfrac{2f_{11}b\lambda}{r}y - Wb\lambda\psi = 0 \end{cases} \tag{4}$$

Applying the numerical calculation method to the simulation run of equation (4), choosing the parameters of table 1 to substitute, so that $y_1 = y, y_2 = \psi; y_3 = \dot{y}_1, y_4 = \dot{y}_2$, and converting equation (4) into an equation of state, we have:

$$\begin{cases} \dot{y}_1 = y_3 \\ \dot{y}_2 = y_4 \\ \dot{y}_3 = -\dfrac{1}{1500}\left[\dfrac{7.24}{V}\times10^6 y_3 + 4.81\times10^6 y_1 - 7.24\times10^6 y_2 + f_t(y) - \sin(\omega t)\right] \\ \dot{y}_4 = -\dfrac{1}{1200}\left[\dfrac{4.36}{V}\times10^6 y_4 + 3.07\times10^6 y_2 + 4.02\times10^6 y_1\right] \end{cases} \tag{5}$$

In equation (5) $\sin(\omega t)$ is the added sinusoidal excitation signal, the rail elasticity coefficient $k=1.7\times10^7$ N/m, the wheel-rail clearance η=0.009 m, and the wheel-rail centres coincide, the non-linear part $f_t(y)$ is:

$$f_t(y) = \begin{cases} 1.7\times10^7 (y-0.009) & y > 0.009 \\ 0 & |y| \le 0.009 \\ 1.7\times10^7 (y+0.009) & y < -0.009 \end{cases} \tag{6}$$

The Matlab software is applied to calculate equation (1), and the critical speed is 55.5 m/s when the system is unstable. taking V as 54 m/s and 57 m/s, it can be seen from Figure 3 that when V=54 m/s, the wheel pair traverse gradually becomes smaller and the system tends to be stable; when V=57 m/s, the wheel pair traverse gradually becomes larger and the system tends to be unstable.
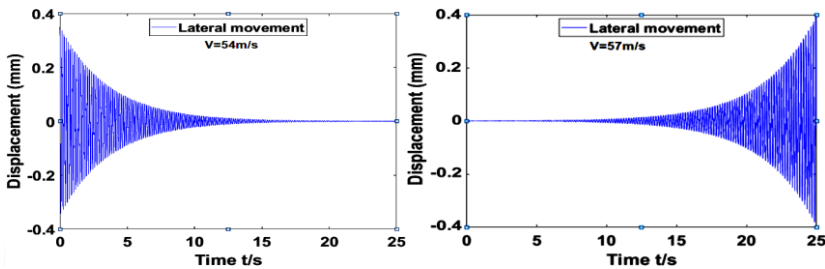

Figure 3. Graph of wheel pair traverse over time at different speeds

A speed V of 55 m/s is chosen and the simulation results are shown in Fig. 4 for 3 Hz, 5 Hz and 10 Hz sinusoidal excitation signals, respectively, without and with rim non-linearity.
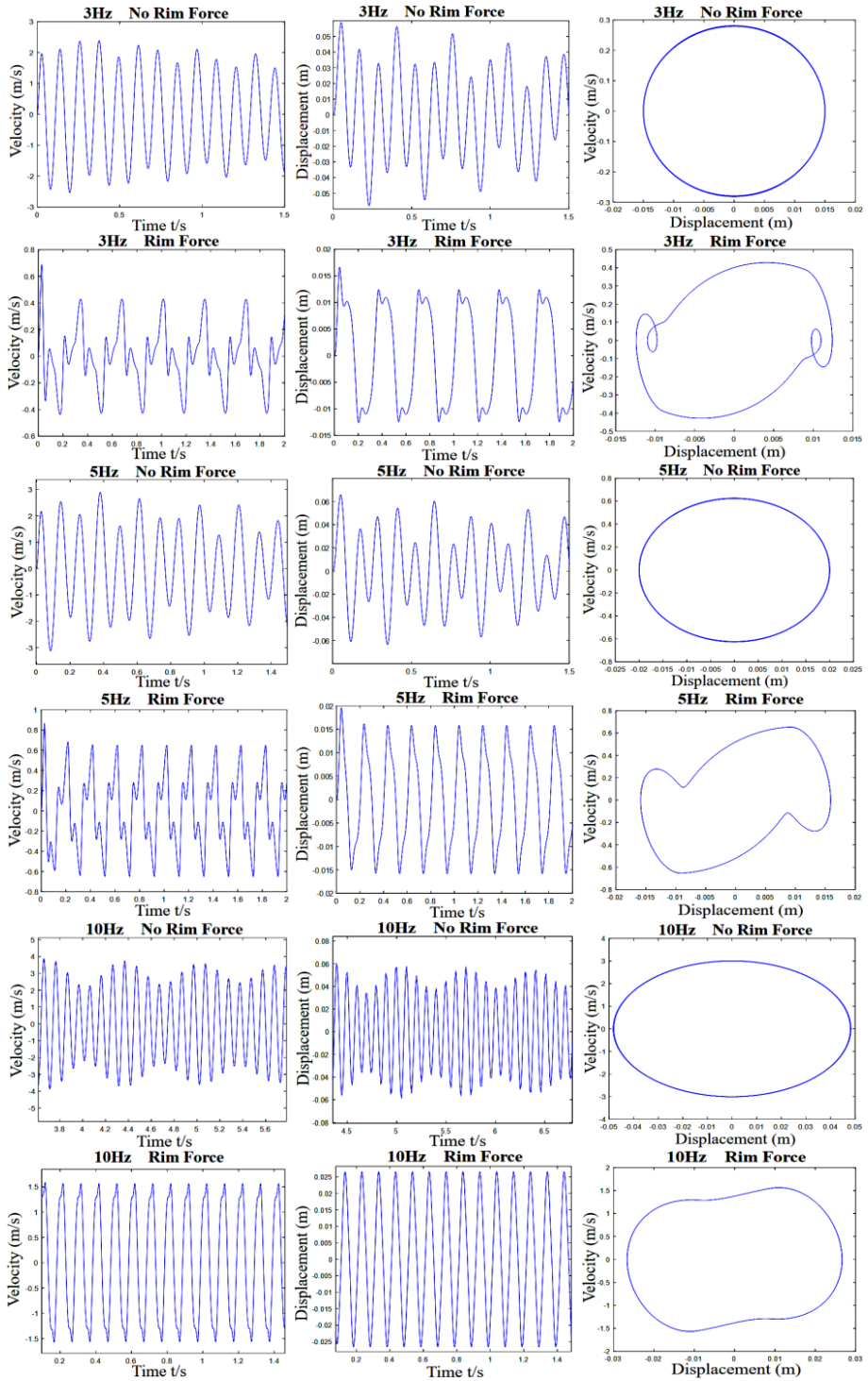
Figure 4. Numerical simulation with non-linear rim forces (V=55 m/s)

As can be seen from Figure 4, when the rim forces are not considered, the simulation results for velocity, displacement and phase diagram do not differ much in shape under three different frequencies of track excitation, but the actual lateral displacement of the wheel pair is by now far beyond the transverse range of the rim, indicating that the application of linear analysis has lost its practical significance. When considering the case of non-linear force intervention at the wheel rim, the wheel pair under 3Hz excitation has a strong collision effect with the track during transverse motion and there is a rebound after the collision, resulting in a continuous collision between the wheels and the track. As the excitation frequency increases, the phenomenon of elastic displacement of the track becomes more pronounced. When the excitation frequency reaches 10Hz, the track tilts sideways, which has a serious impact on the safety of the traffic. Therefore, the critical speed of the vehicle must be reduced when considering the non-linear forces on the wheel edge in order to ensure safe driving.

4. Circuit Design and Multsim 14.0 Simulation

In order to make the kinetic model and the circuit model fully equivalent, the kinetic differential equation should first be converted into an equivalent circuit equation. The output signal of the equivalent circuit simulation is the result of mathematical operations such as addition, subtraction or differentiation and integration of the input signal using capacitors, resistors and operational amplifiers, so the kinetic equation in equation (5) can be rewritten into the following integral form:

$$
\begin{cases}
y_1 = \dfrac{1}{R_1 C_1} \int y_3 \, dt \\[2mm]
y_2 = \dfrac{1}{R_2 C_2} \int y_4 \, dt \\[2mm]
y_3 = \int \left(-\dfrac{1}{R_{31} C_3} y_1 + \dfrac{1}{R_{32} C_3} y_2 - \dfrac{1}{R_{33} C_3} y_3 - \dfrac{1}{R_3 C_3} f_t(y) + \dfrac{V}{R_{17} C_3} \sin(\omega t) \right) dt \\[2mm]
y_4 = \int \left(-\dfrac{1}{R_{41} C_4} y_1 - \dfrac{1}{R_{42} C_4} y_2 - \dfrac{1}{R_{44} C_4} y_4 \right) dt
\end{cases}
\tag{7}
$$

V in Eq. (7) is the output amplitude of the function generator, $\sin(\omega t)$ is the sinusoidal excitation signal and $F_t(y)$ is the segmented function. To facilitate the application of the nonlinear module in the simulation software Multsim to describe the segmented linear function, $F_t(y)$ is rewritten in absolute terms as the following algebraic equation:

$$
F_t(y) = ky - \frac{1}{2} k \left[|y + \eta| - |y - \eta| \right]
\tag{8}
$$

Substituting the parameters into equation (8), we have:

$$
F_t(y) = 1.7 \times 10^7 \left\{ y - \frac{1}{2} \left[|y + 0.009| - |y - 0.009| \right] \right\}
\tag{9}
$$

Four integration modules are selected to implement the circuit equations, and the operational amplifier is selected as TL074CN. The design circuit is shown in Figure 5. The first equation in equation (7) is implemented by U1A and U1B; the second equation is implemented by U2A and U2B; the third equation is implemented by U1C and U1D; and the fourth equation is implemented by U2C and U2D. Where R3 is the non-linear series equivalent resistance, the intervention of the non-linear action of the system is achieved by the closure of switch S1. The function generator XFG1 generates the excitation signal and sets its output signal to be a sinusoidal wave. As track unevenness is an important source of excitation causing vibration in the vehicle system, a resistor R17 of equal resistance to resistor R31 is added to the circuit and connected in series with the sinusoidal excitation signal. The oscilloscope XSC1 is used to read the final output signals y1 and y3, where y1 represents the transverse displacement and y3 the transverse velocity.
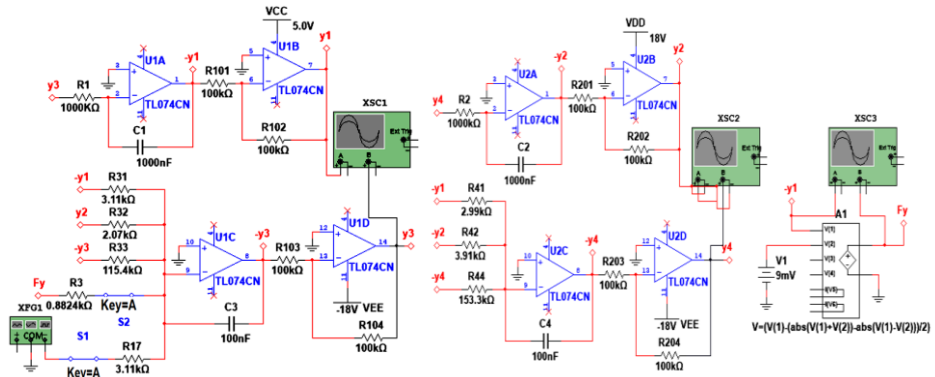

Figure 5. Equivalent circuit model for a single-axis bogie with segmented linearity

A speed of 55m/s, an excitation signal amplitude of 40mV and frequencies of 3Hz, 5Hz and 10Hz were chosen as the disturbance signals, when the line was in a state of self-excited oscillation, as shown in Figure 6 for the effect on the displacement and speed of the wheel pair's lateral movement before and after the intervention of the rim force.
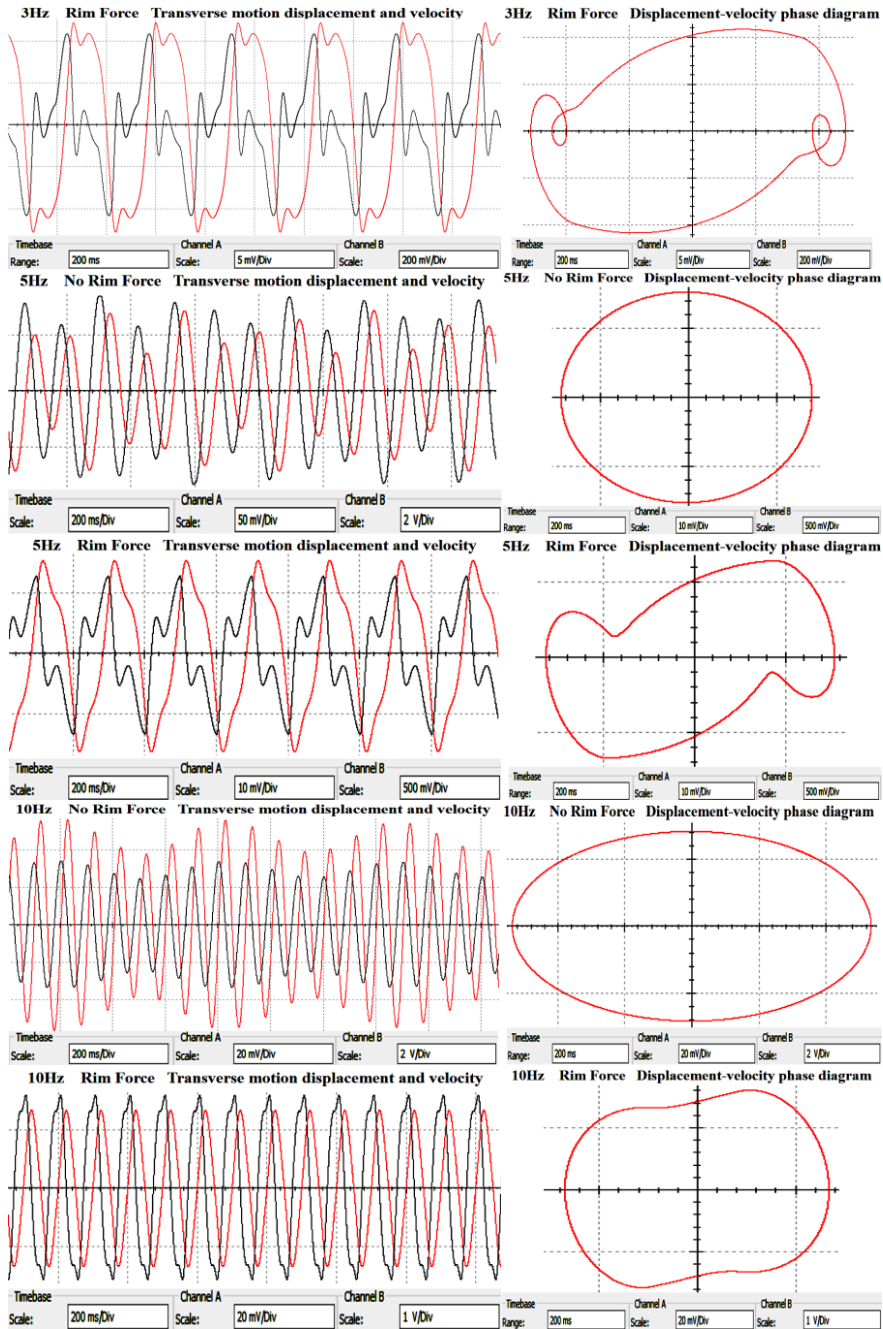
Figure 6. Non-linearity due to rim forces

(transverse motion displacement in red, velocity in black)

As can be seen in Figure 6, the results of both the equivalent circuit simulation and the Matlab numerical simulation are consistent in terms of waveform, amplitude and frequency, verifying that the equivalent circuit model is fully relevant to the study of

vehicle system dynamics. The advantage of the equivalent circuit simulation is that the signal parameters can be adjusted in real time by the signal generator as the output signal changes, which increases the overall speed of the calculation compared to the numerical simulation where the program has to be re-assigned each time. In addition, the parameters can be dynamically modified during the circuit simulation process and the signal changes can be dynamically observed, which is not possible with numerical simulation.

5. Conclusion

The kinetic equations for the elastic wheel pair are established by modelling a single-axle bogie containing non-linear factors. Multisim 14.0 was applied to build a linear circuit model equivalent to the dynamics model, and the non-linear part was added directly to the signal input part according to the mathematical equations. The effect of wheel edge non-linearity on the stability of the vehicle system was analysed and investigated, and the comparison found that the results of the equivalent circuit simulation and the Matlab numerical simulation were consistent, indicating that by adding the non-linear part directly to the linear circuit model on the basis of the The analysis of the dynamics of the non-linear mechanical system can be achieved by adding non-linear inputs directly to the linear circuit model. Equivalent circuit simulation bypasses the complexity of numerical simulation to analyse non-linear systems by adding non-linear factors through visualisation. It has the advantages of modular design, high visualisation, flexible and convenient input and output, ready parameter adjustment and addition of non-linear factors, and simplicity of implementation. At the same time, as the equivalent circuit model can be modified in real time during the simulation, when the parameters change significantly, the Equivalent circuit simulation can also reveal patterns that are not easily detected by numerical simulation, providing a viable tool for the study of dynamics.

References

[1]   Akhmet, M.; Fen, M.O. Extension of Lorenz unpredictability. *International Journal of Bifurcation and Chaos* **2015**, *25*, 1550126. DOI:10.1142/s0218127415501266.
[2]   Leonov, G.A. Shilnikov chaos in Lorenz-like systems. *International Journal of Bifurcation and Chaos* **2013**, *23*, 1350058. DOI:10.1142/s0218127413500582.
[3]   Costamagna, E. A tentative effort to model hunting behaviors of some old locomotives by means of simple non linear circuit equations. In Proceedings of the 2014 Complexity in Engineering (COMPENG), Barcelona, Spain, **2014**; pp. 1-6.
[4]   Sordi, A. Chua's oscillator: An introductory approach to chaos theory. *Revista Brasileira de Ensino de Física* **2021**, *43*, e20200437. DOI:10.1590/1806-9126-rbef-2020-0437.

[5]   Suresh, K.; Palanivel, J.; Thamilmaran, K. Successive torus doubling and birth of strange non-chaotic attractors in non-linear electronic circuit. *Electronics Letters* **2017**, *53*, 1464-1466. DOI:10.1049/el. 2017.1987.

[6]   Ignatyev, A.O.; Ignatyev, O. Quadratic forms as Lyapunov functions in the study of stability of solutions to difference equations. *Electronic Journal of Differential Equations* **2011**, *2011*, 1-21. DOI:10.1016/j.jmaa.2010.09.020.

[7]   Kamiyama, K.; Komuro, M.; Endo, T.; Aihara, K. Classification of bifurcations of quasi-periodic solutions using lyapunov bundles. *International Journal of Bifurcation and Chaos* **2014**, *24*, 1430034. DOI:10.1142/s0218127414300341.

[8]   Loria, A.; Panteley, E. Stability, as told by its developers. *IFAC-PapersOnLine* **2017**, *50*, 5219-5230. DOI:10.1016/j.ifacol.2017.08.459.

[9]   Constantinescu, R.-L.; Roman, M.; Selişteanu, D. Simplified numerical methods used for the approximations of chaotic solutions of dynamical systems. In Proceedings of the 2017 18th International Carpathian Control Conference (ICCC), Sinaia, Romania, **2017**; pp. 560-564.

[10] Zhao, Y.; Zhao, Y.; Li, J.; Chen, Y.; Ren, Q.; Mao, L. Vibration mechanics virtual simulation system based on MATLAB. In Proceedings of the Proceedings of the 28th Annual Conference of Beijing Power Society, Beijing, **2022**; pp. 70-73.

[11] Furch, J. A model for predicting motor vehicle life cycle cost and its verification. *Transactions of FAMENA* **2016**, *40*, 15-26.

[12] Wang, Z. Research on lateral stability of vehicle based on equivalent circuit model. Lanzhou Jiaotong University, Lanzhou, **2022**.

[13] Liu, R.; Wang, Z.; Luo, F. Simulation of the equivalent circuit of two degrees of freedom collision vibration system with gap. *Journal of Mechanical Strength* **2022**, *44*, 53-58. DOI:10.16579/j.issn.1001. 9669.2022.01.007.

[14] Chang, F.; Wang, Z.; Hu, G. Circuit simulation of 2-DOF vibration system with symmetric clearance. *Noise and Vibration Control* **2021**, *41*, 41-45. DOI:10.3969/j.issn.1006-1355.2021.03.007.

[15] Zhang, T.; Dai, H. On the nonlinear dynamics of a high-speed railway vehicle with nonsmooth elements. *Applied Mathematical Modelling* **2019**, *76*, 526-544. DOI:10.1016/j.apm.2019.06.027.

[16] Wang, P.; Yang, S.; Liu, Y.; Liu, P.; Zhao, Y.; Zhang, X. Investigation of stability and bifurcation characteristics of wheelset nonlinear dynamic model. *Chinese Journal of Theoretical and Applied Mechanics* **2022**, *55*, 462-475.

[17] Uyulan, C.; Gokasan, M.; Bogosyan, S. Hunting stability and derailment analysis of the high-speed railway vehicle moving on curved tracks. *International Journal of Heavy Vehicle Systems* **2019**, *26*, 824-853. DOI:10.1504/ijhvs.2019.102685.

[18] Hou, L.; Peng, Y.; Sun, D. Dynamic analysis of railway vehicle derailment mechanism in train-to-train collision accidents. *Proceedings of the Institution of Mechanical Engineers, Part F: Journal of Rail and Rapid Transit* **2021**, *235*, 1022-1034. DOI:10.1177/0954409720959870.

[19] Kalinowski, D.; Szolc, T.; Konowrocki, R. The new simulation approach to tramway safety against derailment evaluation in term of vehicle dynamics. In *TRANSBALTICA XI: Transportation Science and Technology: Proceedings of the International Conference TRANSBALTICA*, Gopalakrishnan, K., Prentkovskis, O., Jackiva, I., Junevičius, R., Eds.; Springer: **2020**; pp. 245-254.

[20] Du, Z.; Wen, X.; Zhao, D.; Xu, Z.; Chen, L. Numerical analysis of partial abrasion of the straddle-type monorail vehicle running tyre. *Transactions of FAMENA* **2017**, *41*, 99-112. DOI:10.21278/TOF.41109.

[21] Kumar, V.; Rastogi, V.; Pathak, P.M. Modelling and evaluation of the hunting behaviour of a high-speed railway vehicle on curved track. *Proceedings of the Institution of Mechanical Engineers, Part F: Journal of Rail and Rapid Transit* **2019**, *233*, 220-236. DOI:10.1177/0954409718789531.

[22] Piotrowski, J.; Bruni, S.; Liu, B.; Di Gialleonardo, E. A fast method for determination of creep forces in non-Hertzian contact of wheel and rail based on a book of tables. *Multibody System Dynamics* **2019**, *45*, 169-184. DOI:10.1007/s11044-018-09635-3.

[23] Sun, Y.; Ling, L. An optimal tangential contact model for wheel-rail non-Hertzian contact analysis and its application in railway vehicle dynamics simulation. *Vehicle System Dynamics* **2022**, *60*, 3240-3268. DOI:10.1080/00423114.2021.1942078.

[24] Wang, Z.; Lei, Y.; Wang, S.; Luo, F. Analysis of dynamic equivalent circuit model of single axle bogie. In Proceedings of the 2021 2nd International Conference on Computer Engineering and Intelligent Control (ICCEIC), Chongqing, China, **2021**; pp. 177-180.

[25] Xie, X.; Wen, S.; Feng, Y.; Onasanya, B.O. Three-Stage-Impulse Control of Memristor-Based Chen Hyper-Chaotic System. *Mathematics* **2022**, *10*, 4560. DOI:10.3390/math10234560.